

STUDY OF ENERGY DEPENDENCE OF PROTON-INDUCED FISSION CROSS SECTIONS FOR HEAVY NUCLEI IN THE ENERGY RANGE 200–1000 MeV

L.A. Vaishnene, V.G. Vovchenko, Yu.A. Gavrikov, A.A. Kotov, V.V. Polyakov, M.G. Tverskoy, O.Ya. Fedorov, Yu.A. Chestnov

The need for the information concerning fission reactions induced in heavy nuclei by intermediate energy projectiles has been obvious. The interest in this process emerges from both fundamental and applied problems of nuclear physics. In spite of extensive experimental efforts, the fission process of nuclei induced by intermediate energy projectiles remains insufficiently understood in many aspects. The proposed measurements of the energy dependence of total fission cross sections of heavy nuclei induced by intermediate energy protons will add to our understanding of the fission process in terms of nuclear properties of highly excited nuclei, such as temperature dependence of level density and fission barriers of excited nuclei. For physics applications, the nuclear data are required for new energy production concepts with the help of accelerator driven system (ADS), for nuclear waste transmutation technologies, for accelerator and cosmic device radiation shields. All the above-mentioned problems require fission cross section data of high accuracy and reliability. Unfortunately, most of experimental data have been obtained in various experiments by using different methods of registration. That is why available data on the fission cross section are dispersed in the range which exceeds the declared accuracy of measurements, not allowing to determine reliable energy dependence of the fission cross section on proton energy. High accuracy of the fission cross section measurements may be achieved only by the use of modern electronic methods of the registration of the both fission fragments in coincidence together with high precision monitoring of a proton flux on the studied target. In the present experiment the method based on the use of gas parallel plate avalanche counters for the registration of complementary fission fragments in coincidence and a telescope of scintillation counters for direct counting of the incident protons on the target has been applied. This method allowed us to measure the absolute proton induced fission cross sections of ^{239}Pu , ^{237}Np , ^{238}U , ^{235}U , ^{233}U , ^{232}Th , ^{209}Bi and $^{\text{nat}}\text{Pb}$ in the energy range from 200 to 1000 MeV with the step of 100 MeV, and results on the energy dependence of total fission cross sections are presented.

The experiment has been performed at 1-GeV PNPI synchrocyclotron. Since an external proton beam of the PNPI synchrocyclotron has a fixed energy of 1 GeV, in order to obtain proton beams with energies in the range from 200 to 900 MeV a method of energy decrease by the beam absorption in a copper degrader was applied [1]. The proton energy was measured by the time-of-flight method. The TOF spectra analysis showed that π^{\pm} mesons were practically absent. The beam diameter at the target chamber location for all proton energies did not exceed 40 mm. The beam profile was measured by a thin scintillation counter which scanned the beam in two orthogonal directions. The beam divergence was determined by measuring the beam profile at the chamber inlet, outlet and in its center at each proton energy variation. The beam intensity distribution on the target was a bi-dimensional normal distribution with the FWHM not larger than ~18 mm.

In the present experiment the fission fragment detector comprised an assembly of two identical gas parallel plate avalanche counters (PPAC) with the target to be studied in between. The PPAC had a high efficiency for the fragment detection and good time characteristics (better than 300 ps time resolution for fission fragments). The latter property, together with the PPAC insensitivity to neutrons, photons and light charged particles with minimal energy loss in the matter, makes the PPACs extremely favorable tool for accelerator experiments, allowing one to place them in the direct proton beam, that provides the large solid angle for the fragment registration ¹.

The PPAC pulse amplitude is determined both by the specific energy losses of the detected particles in heptane and by the gas amplification value. The latter depends on the voltage value between the anode and cathode, so the detection efficiency could be controlled by voltage choosing. By the appropriate choice of the

¹ A.A. Kotov, W. Neubert, L.N. Andronenko, B.L. Gorshkov, G.G. Kovshevy, L.A. Vaishnene and M.I. Yazikov, Nucl. Instr. Meth. **178**, 55 (1980).

voltage value one can introduce a threshold selection criterion which is especially important when detecting the fission fragments from nuclei with a high level of α -activity, such as ^{233}U , ^{237}Np and ^{239}Pu .

Nevertheless, it is not sufficient to employ only the threshold selection criterion when using the PPAC directly in the proton beam. In fact, the amplitude spectrum of the detected particles contains, together with the fission fragments, a considerable contribution of low-amplitude background events. These events are caused by various proton-induced nuclear reactions in the matter along the beam line. Such a low-energy component is strongly suppressed after a coincidence criterion is switched on. Moreover, the analysis of amplitude correlations of the coinciding fragments allowed us to exclude all background events almost thoroughly.

Thus, in our experiment we used three criteria to select the binary fission events: the threshold criterion, the coincidences, and the criterion of the total kinetic energy of detected coincident particles (the amplitude correlations).

The PPAC is so thin that it does not harm practically the beam characteristics when located into the beam. For this reason several assemblies with various targets could be readily placed into the beam. This allowed us to diminish considerably the measurement time. In the real experiment up to six assemblies were used simultaneously. The layout of the setup including the reaction chamber with the fission event detectors and proton monitoring system is shown in Fig. 1. The main part of the setup is a hermetic chamber with six detector assemblies, each assembly comprising the two PPACs and the target in between.

Before entering the reaction chamber the proton beam passed three scintillation counters (S1&S2&S3), combined *via* the coincidence scheme and performed direct proton counting. Just downstream of the reaction chamber the polyethylene target (CH_2)_n was placed. The protons elastically scattered from this target were detected by a two-arm scintillation telescope (S4&S5&S6), which served as a secondary beam monitor.

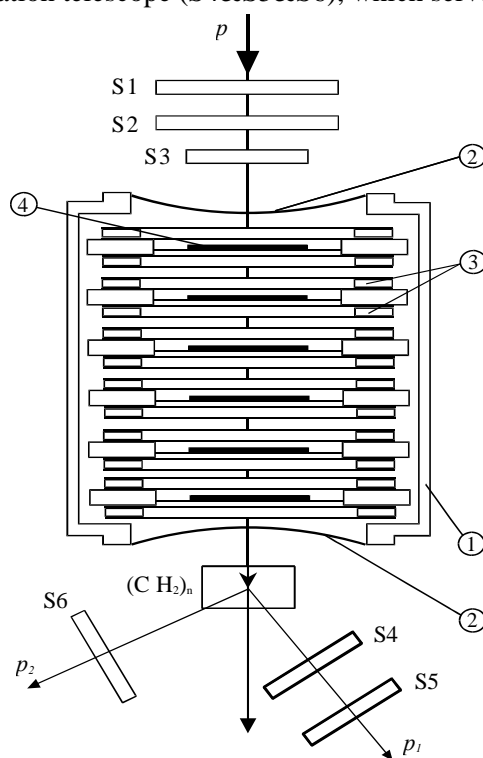


Fig. 1. Experimental setup: 1 – chamber filled with heptane; 2 – entrance window; 3 – PPACs, 4 – target; S1, S2, S3, S4, S5, S6 – scintillation counters

Direct counting of the incident protons with a scintillation counter telescope was used for beam monitoring. This method provides good monitoring accuracy only for low intensity beams, up to $\sim 10^5 \text{ s}^{-1}$. However, for bismuth and lead nuclei with the fissionability is about an order of magnitude lower than for actinide nuclei one needs much higher intensity. For this reason the measurements were performed at two intensity values of

the proton beam: $\sim 10^5 \text{ s}^{-1}$ and $10^6\text{--}10^7 \text{ s}^{-1}$. In the latter high intensity case the beam monitoring was done by two methods: 1) by detecting the fission events from the calibration target of ^{238}U residing in the reaction chamber, and 2) by detecting the events of the pp scattering on the auxiliary $(\text{CH}_2)_n$ target with the two-arm scintillation telescope (S4&S5&S6). Both methods were previously calibrated at low intensity ($< 2 \times 10^5 \text{ s}^{-1}$) with the direct monitoring telescope (S1&S2&S3). The comparison of both methods at high intensity showed the agreement of results within $\sim 3\%$ at all energies from 200 to 1000 MeV. The calibration procedure for secondary monitoring is described in detail in Ref. [2].

The target to be investigated was a thin layer of material laid by vacuum evaporation on a thin 50 mm in diameter backing foil made of alumina (Al_2O_3). The thickness of actinide targets, their composition and the uniformity of the evaporated layer were determined by measuring the α -activity and energy spectra of the α -particles. For the lead and bismuth targets the thickness of the backings and targets was determined by measuring the energy losses of α -particles passing through the target.

So, using the methods of detection of the binary fission events and beam monitoring described in Ref. [2] we have measured the fission cross sections for each target at nine proton energies.

The cross section calculation procedure comprised the following steps.

1. Background subtraction after the analysis of the bi-dimensional amplitude distribution of the detected events. The number of the background events amounted to 2–3% of the total number of the detected events.
2. Determination of the solid angle for the fission event detection for each assembly. The calculation was done by a Monte Carlo simulation which took into account: the proton beam profile on the target; the detection geometry for the fission fragments, their mass and energy distributions as well as the anisotropy of fragment angular distribution in the laboratory frame due to the longitudinal momentum component of the fissioning nucleus. The statistical accuracy of the solid angle calculations amounted to 0.1%.
3. Estimation of the undetectable portion of the fission events caused by the energy loss of the fission fragment in the target, its backing and in the PPAC electrodes. The undetectable part of the events depended on the target nucleus and thickness and amounted to 3–8%.
4. Determination of the integral proton flux through the target, with the account of the scintillation telescope efficiency and the probability of the appearance of more than one proton in a microbunch at low intensity.
5. Determination of the normalizing coefficients to calculate the proton flux at high intensity *via* the counting rate of the pp -scattering monitor and the fission counting rate from the calibration target.

The measured fission cross sections for ^{239}Pu , ^{237}Np , $^{233,235,238}\text{U}$, ^{232}Th , ^{209}Bi and $^{\text{nat}}\text{Pb}$ nuclei are shown in Table. For the most of nuclei the data presented are averaged over the results of several measurements, the errors being determined mainly by the monitoring errors and the uncertainty in the target thickness.

The energy dependence of the fission cross sections obtained in the present experiment for the mentioned nuclei is shown in Fig. 2. Also presented are the results of previous experiments extracted from compilations ^{2,3} as well as the JINR data on the fission of ^{237}Np , $^{235,238}\text{U}$, ^{232}Th and ^{209}Bi nuclei induced by 1000 MeV protons. In the compilation ² a parameterization of all the world fission cross section data was proposed after the critical analysis and data selection for the actinide and pre-actinide nuclei for proton energies up to 10–30 GeV. The results of this cross section estimation are also given in Fig. 2 by dashed lines.

As seen in Fig. 2, the energy dependence of the fission cross sections for all actinide nuclei is characterized by common regularities demonstrating the rise of the cross sections in the energy range from 200 to ~ 400 MeV with the following plateau up to 1000 MeV. Such a behavior is not consistent with estimations of compilation ² (dashed lines) which predict smooth decrease of the cross sections with energy in the range 200–1000 MeV. Our experimental results for actinide nuclei together with the previously available data at low energies (below 200–300 MeV) form a certain picture of the energy behavior of the fission cross sections in the whole energy range from the threshold up to 1000 MeV. In fact, a large body of the data indicates (at least for ^{237}Np , ^{238}U , ^{235}U and ^{232}Th nuclei) the presence of the maximum in the energy dependence near several tens MeV, followed by the cross section decrease up to the energy of ~ 200 MeV. Then after the indistinct minimum near 200–300 MeV the cross sections rise again till

² A.V. Prokofiev, Nucl. Instr. Meth. A **463**, 557 (2001).

³ A.I. Obukhov, Particles & Nuclei **32**, 319 (2001).

~ 400 MeV reaching a plateau which continues up to the maximum energy of 1000 MeV. The change of the energy behavior of the fission cross sections near 200 MeV resembles a characteristic minimum of the total inelastic cross section of the proton-nucleus interaction in the same energy region.

Table

Fission cross sections, mb

Energy, MeV	²³⁹ Pu	²³⁷ Np	²³⁸ U	²³⁵ U
207	1260 ±126	1187 ± 81	1352 ± 68	1464 ± 83
302	1339 ±134	1438 ± 98	1470 ± 68	1562 ± 94
404	1585 ±158	1624 ± 88	1527 ±104	1626 ±138
505	1613 ±161	1607 ± 98	1491 ± 78	1592 ±102
612	1628 ±163	1647 ±100	1499 ± 72	1610 ±124
702	1700 ±170	1674 ±102	1518 ± 76	1620 ±131
802	1672 ±167	1629 ± 88	1503 ± 63	1571 ± 90
899	1688 ±168	1673 ±114	1490 ± 63	1592 ± 96
1000	1592 ±159	1568 ± 96	1489 ± 64	1591 ±113
Energy, MeV	²³³ U	²³² Th	²⁰⁹ Bi	^{nat} Pb
207	1625 ±162	1144 ± 90	136 ± 13	60.5 ± 3.5
302	1651 ±115	1200 ± 91	178 ± 17	84 ± 4.5
404	1767 ±124	1236 ± 91	207 ± 21	110 ± 6
505	1818 ±123	1239 ± 61	227 ± 23	118.5 ± 6
612	1763 ±123	1268 ± 80	233 ± 23	127 ± 6.5
702	1798 ±126	1285 ± 81	235 ± 23	132.5 ± 9.5
802	1778 ±124	1247 ± 54	229 ± 23	131 ± 8.5
899	1779 ±122	1252 ± 58	239 ± 24	133.5 ± 7.5
1000	1745 ±122	1245 ± 85	235 ± 23	129 ± 8.5

The energy behavior of the cross sections for pre-actinide nuclei ²⁰⁹Bi and ^{nat}Pb demonstrates sharp increase in the range 200–400 MeV changing gradually to plateau at higher energy, at about 500 MeV for ²⁰⁹Bi and ~700 MeV for ^{nat}Pb. Our data for ²⁰⁹Bi nuclei are in a good agreement with the previous experiments in the energy range 200–600 MeV, while for ^{nat}Pb our data in the range 200–400 MeV lie somewhat lower than the previous experimental results.

Theoretical calculations of fission cross sections were carried out [3, 4] in the framework of the two-step cascade evaporation model. At the first stage of the reaction, when the mean range of the incident protons in the nucleus is comparable with the nucleus diameter, the interaction of the nucleon with the nucleus may be considered as a cascade of binary collisions of the incident nucleon with separate nucleons of the initial nucleus. During this fast stage ($\tau \sim 10^{-22}$ s) some part of fast nucleons leaves the nucleus taking away a considerable part of energy. The rest of the energy is transformed into the excitation energy of the residual nucleus which nucleon composition differs from that of the initial nucleus. So, after the cascade stage of the reaction a residual nucleus appears with wide spectra of the nucleon composition and excitation energies, which depend on the incident nucleon energy. At the second (slow) stage of the reaction ($\tau \sim 10^{-16} - 10^{-19}$ s) the highly excited nucleus either emits nucleons or undergoes the fission. The calculation of the cascade stage of the interaction was done by us with the help of the modified version of the model of the intranuclear cascade ⁴, in which a Fermi-gas model of the nucleus was used with the account of the nucleon density spread at the border of the nucleus. This version of the cascade-evaporation model was successfully used earlier to analyze the reactions of deep disintegration and fission ⁵ induced by 1-GeV protons. At the stage

⁴ V.E. Bunakov, M.M. Nesterov and N.A. Tarasov, Phys. Lett. B **73**, 267 (1978).

⁵ L.N. Andronenko, A.A. Kotov, M.M. Nesterov, V.F. Petrov, N.A. Tarasov, L.A. Vaishnena and W. Neubert, Z. Phys. A **318**, 97 (1984).

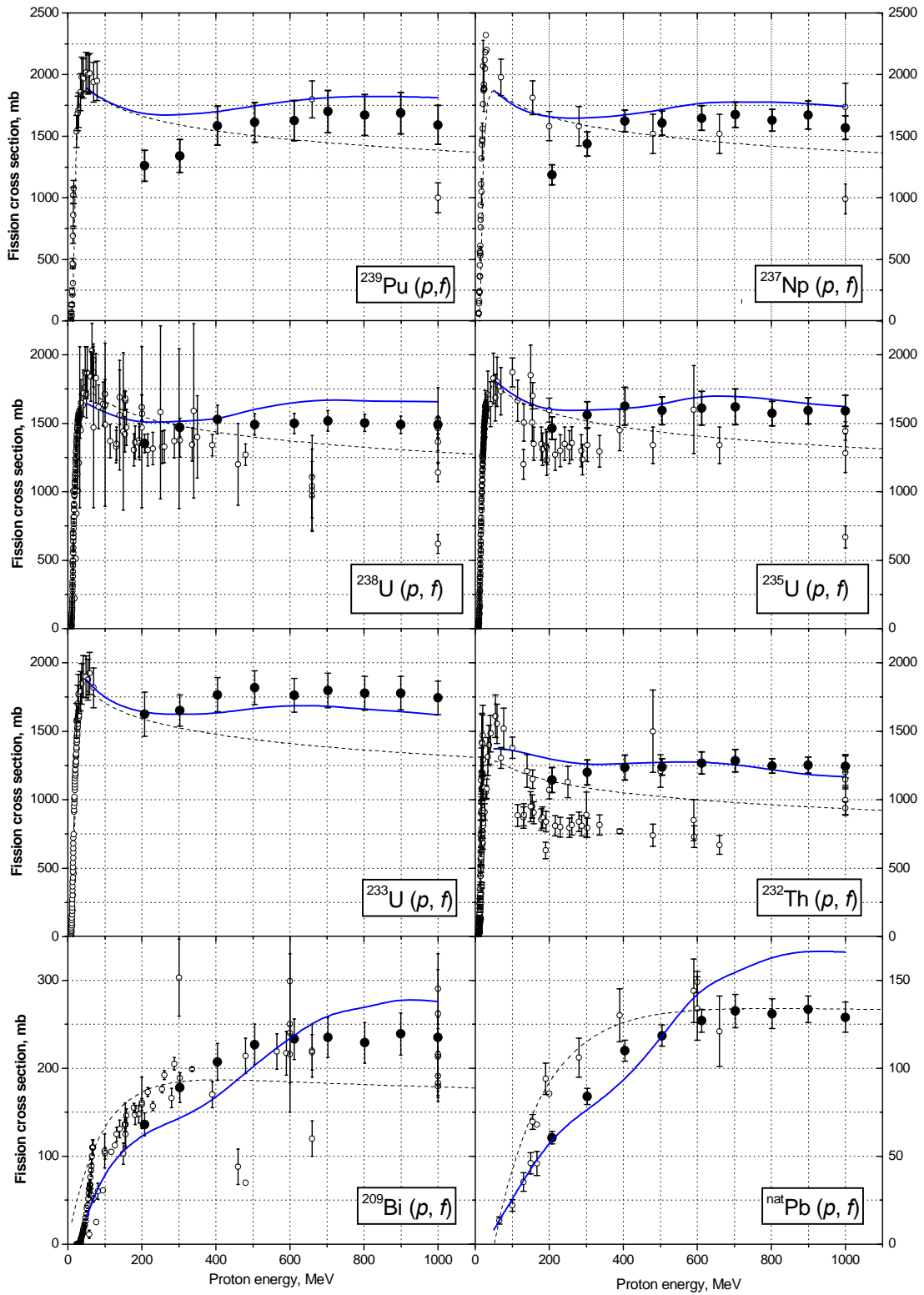


Fig. 2. Energy dependences of the fission cross sections. Black circles – our data, open circles – data from the compilation². Dashed line – parameterization from the compilation², solid line – theoretical calculations

of the decay of the highly excited nucleus the fission cross section is determined mainly by the ratio of the fission probability to the probability of the neutron emission. The probability of the neutron emission was calculated in the frame of the statistical theory of Weisskopf, the fission probability being considered in the Bohr-Wheeler approach. When calculating the fission cross sections, one needs, as a rule, to vary the nuclear level density at the equilibrium deformation a_n and at the saddle point of the fissioning nucleus a_f , as well as the fission barrier value B_f . It was supposed that at high excitation energy nuclear shell effects in the fission barriers may be neglected, the ratio of the level density parameters a_f/a_n being supposed to be independent of the excitation energy of the decaying nucleus. In our calculations the level density parameter a_n was taken to be $A/10 \text{ MeV}^{-1}$ for all actinide nuclei and $A/16$ for pre-actinide nuclei of Bi and Pb, the ratio of the level density parameters a_f/a_n being equal to 1.1. The fission barriers calculated in the liquid drop model were taken for B_f . The results of the calculations are presented by solid lines in Fig. 2. It is seen that the calculations reproduce qualitatively the general behavior of the cross sections in the range 50–1000 MeV, with a minimum near 200–300 MeV and a plateau above 400 MeV for actinide nuclei. However, our experimental data for ^{239}Pu and ^{237}Np at 200 and 300 MeV and for $^{\text{nat}}\text{Pb}$ at 700–1000 MeV lie considerably lower than the calculated cross sections.

The dependences of the total fission cross sections on the parameter Z^2/A of the target nucleus are shown in Fig. 3 at the proton energies of 207 and 1000 MeV. It is seen that the total fission cross section is an increasing function of the Z^2/A parameter only up to ^{233}U nucleus, while for ^{237}Np and ^{239}Pu the cross sections are equal but lower than that for ^{233}U . Besides, the fission cross sections for uranium isotopes in the whole energy range demonstrate systematically (despite considerable experimental uncertainties) the rise of the cross section when going from ^{238}U to lighter isotopes – see Fig. 4.

The isotope dependence of the fission cross sections for uranium was observed earlier in the experiments on the fission induced by neutrons and photons ^{6,7} of intermediate energies. The cross section values for uranium fission induced by neutrons of 100–300 MeV energy are in a good agreement with our data in the corresponding energy region.

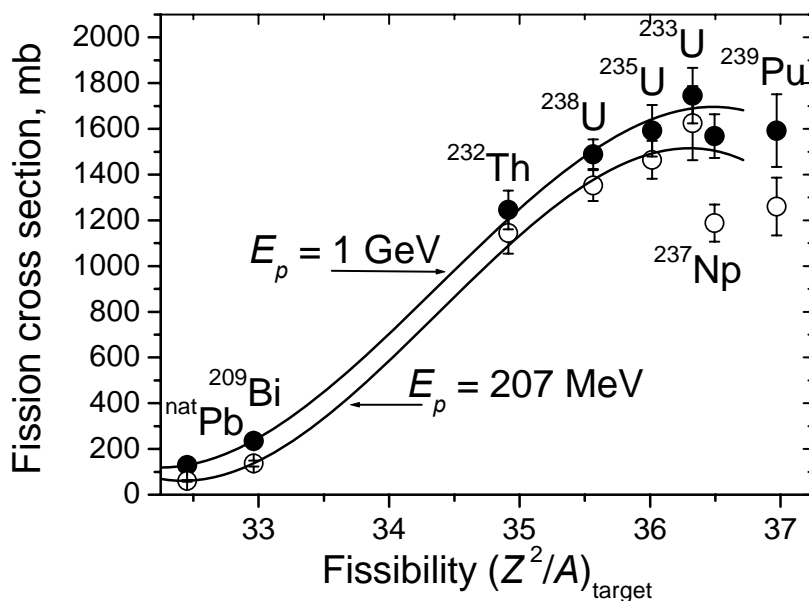


Fig. 3. Dependences of the total fission cross sections on the parameter Z^2/A of the target nucleus

⁶ P.W. Lisowski *et al.*, in *Proceedings of the International Conference on Nuclear Data for Sciences and Technologies* (Juelich, Germany, 13 – 17 May 1991), p. 731.

⁷ J.C. Sanabria *et al.*, *Phys. Rev. C* **61**, 426 (2000).

However, the existence of the isotope dependence of the uranium fission cross sections for higher energies looks unexpected and strange from the point of view of the cascade evaporation model for two reasons. First, as it was written above, the cascade stage of the proton-nucleus interaction results in the formation of the wide isotope spectrum of the residual excited nuclei, that should lead to the "loss of the memory" about the nucleon composition in the input channel reaction (nucleon composition of the initial nucleus).

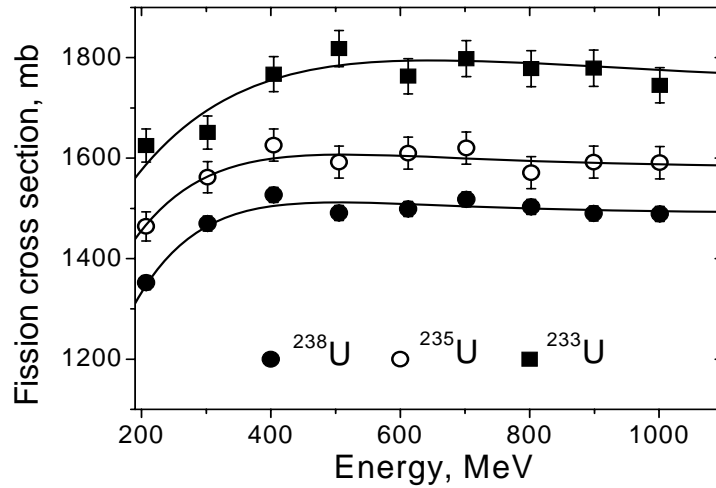


Fig. 4. Fission cross sections for uranium isotopes

Second, the fission barriers B_f for the uranium nuclei calculated in the liquid drop model amount to less than 10 MeV, the difference in the B_f values for a series of the residual nuclei not exceeding several MeV. So the version of the cascade evaporation model we used cannot reproduce the isotopic dependence of the fission cross sections for uranium nuclei.

The analysis of the dependence of the total fission cross sections on the parameter Z^2/A of the actinide nucleus in proton energy region of 200–1000 MeV shows that decreasing uranium mass number on one neutron or proton is accompanied by changing the fission cross section by ~3%. The fission cross sections increase or decrease proportionally to the parameter Z^2/A (Fig. 5).

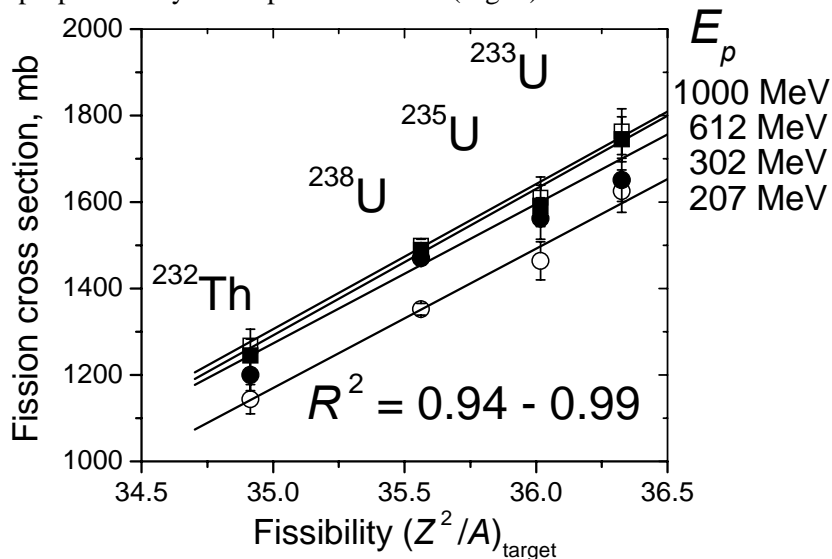


Fig. 5. Dependences of the fission cross sections on the parameter Z^2/A for various energies

To resume, we can formulate a summary.

For the first time in one and the same experimental technique the cross sections of proton-induced fission for ^{nat}Pb , ^{209}Bi , ^{232}Th , ^{233}U , ^{235}U , ^{238}U , ^{237}Np and ^{239}Pu nuclei have been measured in the wide energy range from 200 to 1000 MeV. The analysis of the results and comparison with the previous experimental data allows one to come to the following conclusions.

The cross sections for all actinide nuclei have similar energy dependences characterized by the rise of the cross sections in the range from 200 to ~400 MeV followed by a plateau which continues up to at least 1000 MeV.

For pre-actinide nuclei Bi and Pb the increase of the cross sections for energies above 200 MeV is faster. The rise then changes to a plateau which begins at ~500 MeV for ^{209}Bi and at ~600 MeV for ^{nat}Pb and continues till 1000 MeV.

The calculations of the fission cross sections in the framework of the cascade evaporation model allow one to reproduce qualitatively the cross section behavior.

The data for uranium isotopes in the whole energy range demonstrate the systematic rise (despite considerable experimental uncertainties) of the cross section when going from ^{238}U to lighter isotopes.

The total fission cross section in the saturation region (at the proton energy of 1000 MeV) is an increasing function of the Z^2/A parameter only up to ^{233}U nucleus, while the cross section values for ^{237}Np and ^{239}Pu are approximately equal to the cross section for ^{235}U .

References

1. N.K. Abrossimov, V.G. Vovchenko, V.A. Eliseev, E.M. Ivanov, Yu.T. Mironov, G.A. Riabov, M.G. Tverskoy and Yu.A. Chestnov, Preprint PNPI-2525, Gatchina, 2003. 31 p.
2. V.G. Vovchenko, L.A. Vaishnene, Yu.A. Gavrikov, A.A. Kotov, V.I. Murzin, V.V. Poliakov, S.I. Trush, O.Ya. Fedorov, Yu.A. Chestnov, A.V. Shvedchikov and A.I. Shchetkovski, Preprint PNPI-2532, Gatchina, 2003.
3. A.A. Kotov, L.A. Vaishnene V.G. Vovchenko, Yu.A. Gavrikov, A.Yu. Doroshenko, V.I. Murzin, V.V. Poliakov, M.G. Tverskoy, O.Ya. Fedorov, T. Fukahori, Yu.A. Chestnov and A.I. Shchetkovski, *Izvestiya RAN, ser. fiz.*, **70**, 1602 (2006).
4. A.A. Kotov, L.A. Vaishnene, V.G. Vovchenko, Yu.A. Gavrikov, V.V. Poliakov, M.G. Tverskoy, O.Ya. Fedorov, Yu.A. Chestnov, A.I. Shchetkovskiy, A.V. Shvedchikov, A.Yu. Doroshenko and T. Fukahori, *Phys. Rev. C* **74**, 034605 (2006).